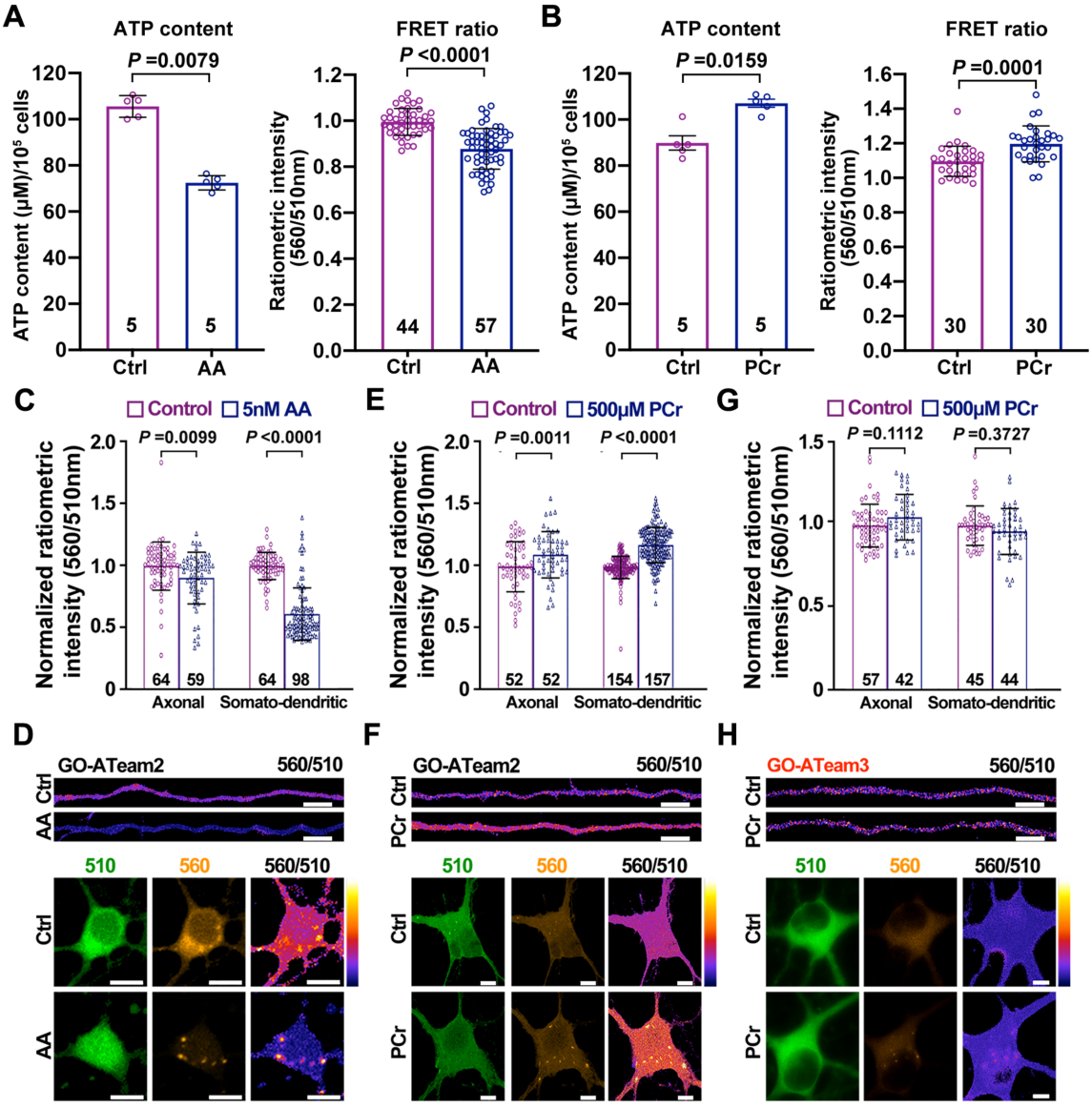

Figure S1 (related to Figure 1). **GO-ATeam2 Is a Sensitive Intracellular ATP Probe in Neurons**

(**A, B**) A non-linear correlation between ATP content (μM/10^5 neurons) and FRET-based ATP assay. Cellular [ATP] was mildly suppressed or elevated by treating cortical neurons (DIV8) with antimycin-A (AA, 1 nM, **A**), an inhibitor of mitochondrial complex III, or phosphocreatine (PCr, 500 μM, **B**), an energy buffering compound, for 24 hours, respectively. Data were quantified from 5 replicate wells in luciferase-based ATP assay or ≥ 30 cell images in FRET-based ATP assay. Note that a small reduction (12%) of the FRET/GFP ratio by 1-nM AA treatment is correlated with a larger (~30%) decline in ATP content (μM/10^5 neurons) (**A**). Similarly, a 10% increase in the FRET/GFP ratio by 0.5-mM PCr treatment corresponds to an ~20% increase in cellular [ATP] within neurons (**B**).

(**C, D**) Quantification (**C**) and representative images (**D**) of axonal (upper) and somatodendritic (lower) intracellular ATP in DIV7 neurons infected with lenti-GO-ATeam2 at plating and treated with control (PBS) or 5 nM AA for 24 hours to reduce ATP while maintaining axon integrity and neuron survival during the live imaging period. Note that the GO-ATeam2 ATP sensor accurately reflects reduced ATP production from mitochondria in both axons ($P = 0.0099$) and somas ($P < 0.0001$) treated with AA.

(**E, F**) Quantification (**E**) and representative images (**F**) of axonal (upper) and somatodendritic (lower) intracellular ATP in DIV7 neurons infected with lenti-GO-ATeam2 at plating and treated with control or phosphocreatine (PCr, 500 μM) for 24 hours. Note that the GO-ATeam2 ATP sensor accurately reflects increased cytoplasmic ATP in axons ($P = 0.0011$) and somas ($P < 0.0001$) treated with PCr.

(**G, H**) Quantification (**G**) and representative images (**H**) of axonal (upper) and somatodendritic (lower) ATP-insensitive GO-ATeam3 signals in DIV7 neurons treated with control or PCr (500 μM) for 24 hours. Note that GO-ATeam3 does not respond to changes in intracellular ATP level in axons ($P = 0.1112$) or somas ($P = 0.3727$) following treatment with PCr.

Data were quantified from the total number of somas or axons (**C, E, G**) indicated in the bars from three biological replicates and expressed as mean ± SD. Statistical analyses were performed using a Mann-Whitney test (ATP content in **A, B**), an unpaired Student's t-test (FRET ratio in **A, B**) or a two-way ANOVA test with Sidak's multiple comparisons test (**C, E, G**). Scale bars, 5 μm (**D, F, H**, upper), 25 μm (**D**, lower), 10 μm (**F**, lower), 5 μm (**H**, lower).

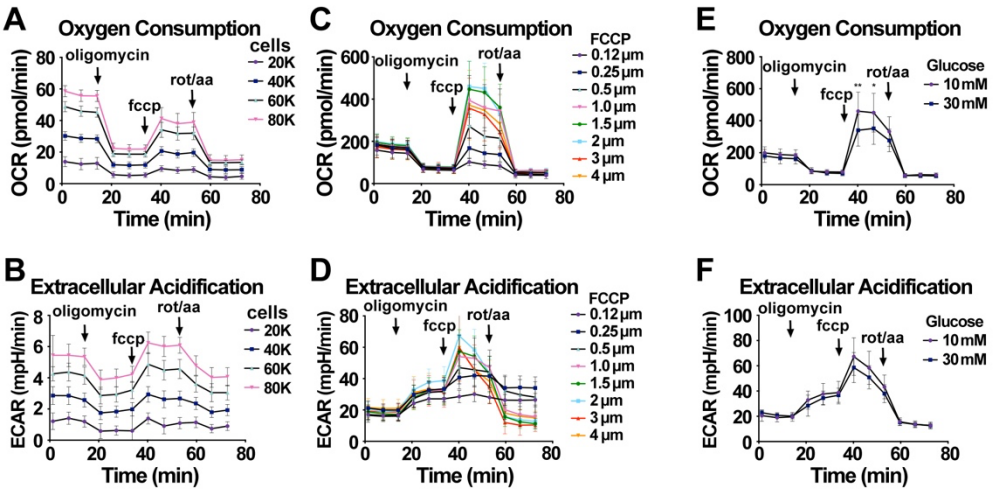

Figure S2 (related to Figure 1). **Optimization of Seahorse Extracellular Flux Analysis**

(**A, B**) Representative traces of oxygen consumption rate (OCR) (**A**) and extracellular acidification rate (ECAR) (**B**) during a single Seahorse Extracellular Flux experiment designed to determine optimal plating density of primary cortical neurons. DIV7 neurons were given a mitochondrial stress test by sequential injections of oligomycin (1 µM), FCCP (1.5 µM), and Rotenone/AA (0.5µM). As OCR was maximal at 80,000 neurons/well, 80,000-100,000 neurons were plated for experiments.

(**C, D**) Representative traces of OCR (**C**) and ECAR (**D**) during a single mitochondrial stress test designed to determine the optimal FCCP concentration. Maximal respiration, determined as peak OCR following FCCP injection, was highest in neurons treated with 2 µM FCCP, thus this treatment concentration was selected for experiments.

(**E, F**) Representative traces of OCR (**E**) and ECAR (**F**) during a single mitochondrial stress test designed to determine the optimal glucose concentration within the Seahorse assay buffer. As maximal respiration was highest in neurons maintained in 10 µM glucose buffer, this concentration was selected for experiments.

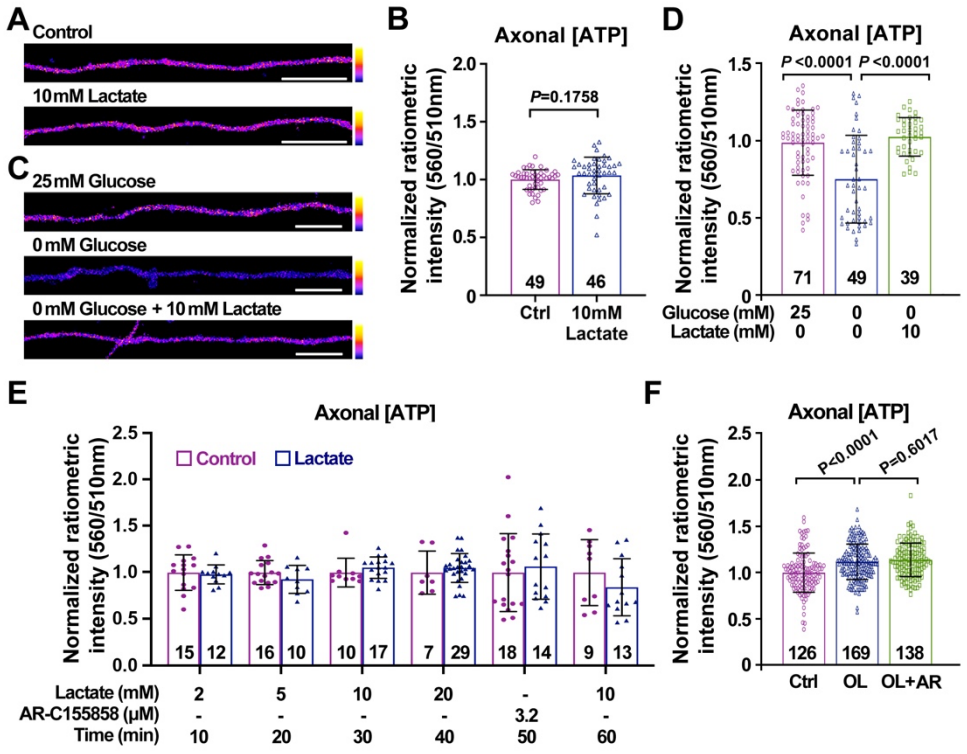

Figure S3 (related to Figure 2)**. Lactate Does Not Mediate the Main Effect of Oligodendrocytes on Axonal ATP Enhancement**

(**A, B**) Representative images (**A**) and quantification (**B**) of axonal ATP of DIV8 neurons infected with lenti-GO-ATeam2 at plating and treated with control (PBS) or L-lactate (10 mM) for 24 hours on DIV7. Note that lactate addition does not enhance cytoplasmic ATP in axons (*P* = 0.1758) maintained in culture media containing 25 mM glucose.

(**C, D**) Representative images (**C**) and quantification (**D**) of axonal ATP of DIV8 neurons maintained in glucose-containing media (25 mM), glucose-free media, or glucose-free media supplemented with 10 mM Lactate. Note that lactate serves as an energy substrate to maintain axonal ATP level when glucose is unavailable.

(**E**) Quantification of axonal ATP of DIV7 neurons treated with increasing concentrations of lactate (2-20 mM) or the lactate transporter blocker AR-C155858 (AR) over time (min). Note that there is no significant difference in axonal ATP between control axons and those treated with increasing concentration of lactate over time.

(**F**) Quantification of ATP in DIV6-8 axons cultured alone (Ctrl), co-cultured with OLs, or co-cultured with OLs combined with the lactate transporter blocker (OL+AR). Note that blocking lactate transport has no impact on OL-mediated enhancement of axonal ATP levels (*P* = 0.6017, OL vs OL + AR).

Data were quantified from the total number of axons indicated in the bars and expressed as mean ± SD. Statistical analyses were performed using an unpaired Student's t-test (**B**) or a one-way ANOVA with Tukey's multiple comparisons test (**D, E, F**). Scale bars, 5 μm.

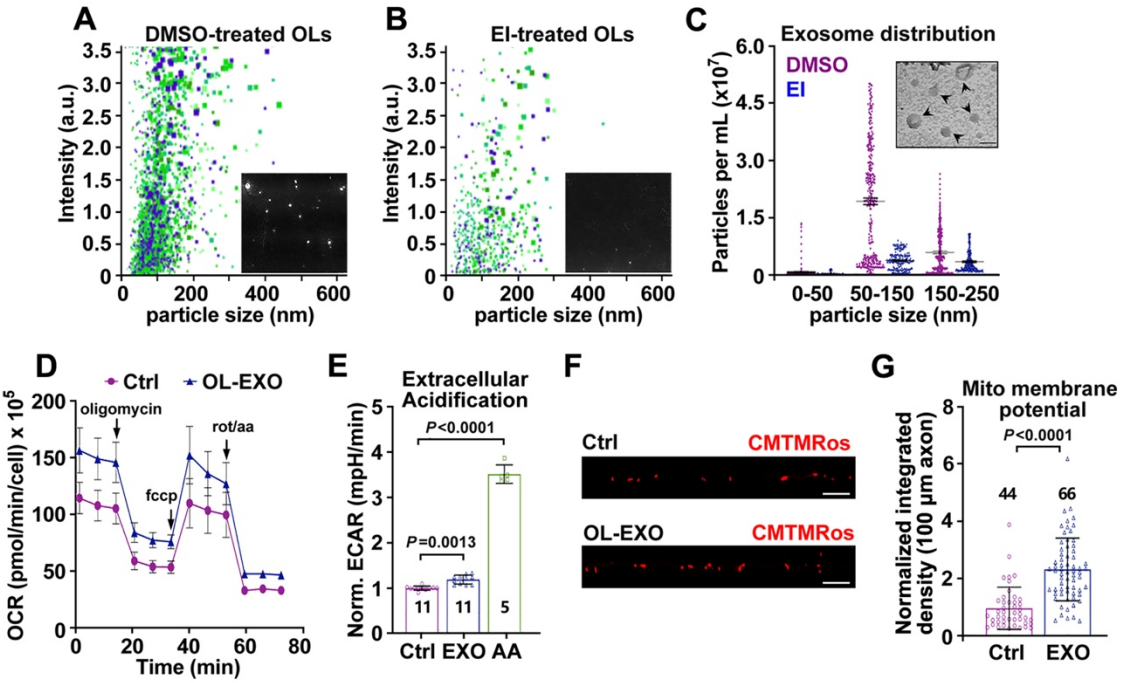

Figure S4 (related to Figure 2). **Exosomes Released from Oligodendrocytes Enhance Axonal Mitochondrial Energetics**

(**A-C**) Nanosight tracking analysis (NTA) of OL-released exosomes. Representative scatter plots show size distribution of nanoparticles derived from DIV2 OLs treated with DMSO as control (**A**) or exosome inhibitor (EI) GW-4869 (1 µM) for 24 hours on DIV1 (**B**). Insets are representative snapshots of light scattering by nanoparticles in each condition (**A, B**). The distribution of particles per ml is shown in **C**, with each data point representing the number of particles of a particular size range (nm) averaged over 5 recordings (60 seconds each, 30 frames per second). Particle sizes have been binned into 0-50, 50-150, and 150-250 nm along the x-axis. Note that the majority of nanoparticles are between 50-150 nm in size, consistent with exosomes. Blocking exosome release with EI reduces exosome-like nanoparticles released from OLs. Inset (**C**) depicts an electron micrograph of exosomes with typical cup-shaped morphology (arrowheads).

(**D**) Representative traces of oxygen consumption rate (OCR) during a single Seahorse Extracellular Flux experiment in which DIV8 neurons were treated with control media (Ctrl) or purified OL-EXOs for 24 hours. A mitochondrial stress test was performed by sequential injections of oligomycin (1µM), FCCP (1.5 µM), and Rotenone/AA (0.5 µM) as indicated. Note that OL-EXOs are sufficient to enhance neuronal mitochondrial bioenergetics similar to OL-CM.

(**E**) Neurons treated with OL-EXOs exhibit increased extracellular acidification (P = 0.0013). As a negative control, neurons were treated with AA (100 nM) for 24 hours.

(**F, G**) Representative images (**F**) and quantification (**G**) showing OL-EXO-mediated enhancement of axonal mitochondrial membrane potential (ψ_m). Axonal chambers were treated with control media (Ctrl) or purified OL-EXO for 24 hours on DIV7 or DIV9, followed by loading of MitoTracker™ Orange CMTMRos (20 nM) for 30 min prior to imaging. Normalized integrated density of CMTMRos signal within individual axonal mitochondria was quantified. Note that axonal

mitochondria display significantly higher ψ_m upon treatment with OL-EXOs ($P < 0.0001$), reflecting enhanced mitochondrial integrity and ATP production capacity.

Data were quantified from the total number of neuronal wells (**E**) or axons (**G**) indicated within or above bars from more than three biological replicates and expressed as mean ± SD. Statistical analyses were performed using a one-way ANOVA test with Tukey's multiple comparisons test (**E**), or an unpaired Student's t-test (**G**). Scale bars, 10 μm (**F**), 100 nm (**C**).

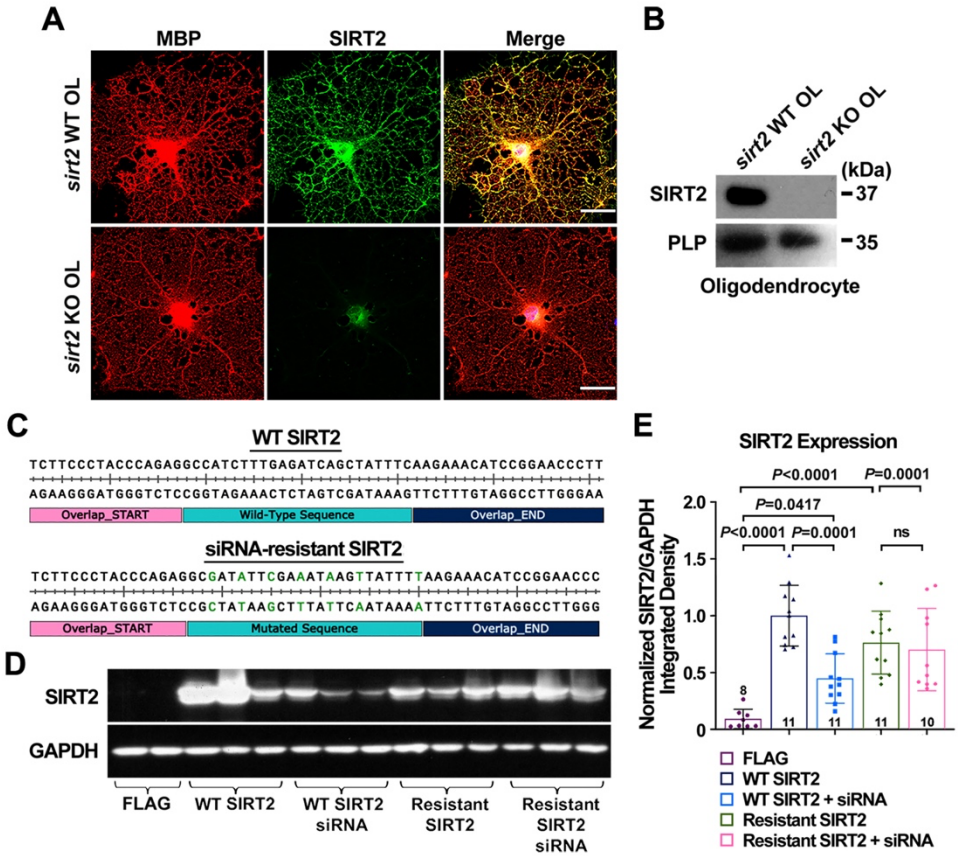

Figure S5 (related to Figure 3 and 5). **Validation of SIRT2 Expression after *sirt2* Deletion or SIRT2 Knockdown**

(**A**) Representative images of DIV10 primary OLs expressing MBP (red) harvested from wild-type (WT) and *sirt2* KO mice. Note that SIRT2 is hardily detectable in *sirt2* KO OLs, indicating the specificity of the anti-SIRT2 antibody.

(**B**) Immunoblots showing loss of SIRT2 expression in *sirt2* KO OLs. Equal amounts (14 μg) of OL cell lysates were loaded and immunoblotted with the indicated antibodies. Note that SIRT2 expression is abolished in *sirt2* KO OLs, which express proteolipid protein 1 (PLP1).

(**C**) Sequence comparison of WT and siRNA-resistant SIRT2, which harbors seven nucleic acid mutations (green) designed to hinder siRNA binding without altering amino acid sequence.

(**D, E**) Representative immunoblots (**D**) and quantification of normalized SIRT2/GAPDH integrated density (**E**) in transfected HEK293T cells. Note that SIRT2-siRNA effectively depletes WT SIRT2 protein level (P = 0.0001), but not siRNA-resistant SIRT2 protein level.

Data were quantified from the total number of cell lysates indicated in or above bars from four biological replicates and expressed as mean ± SD. Statistical analyses were performed using a one-way ANOVA test with Tukey's multiple comparisons test. Scale bars, 25 μm (**A**).

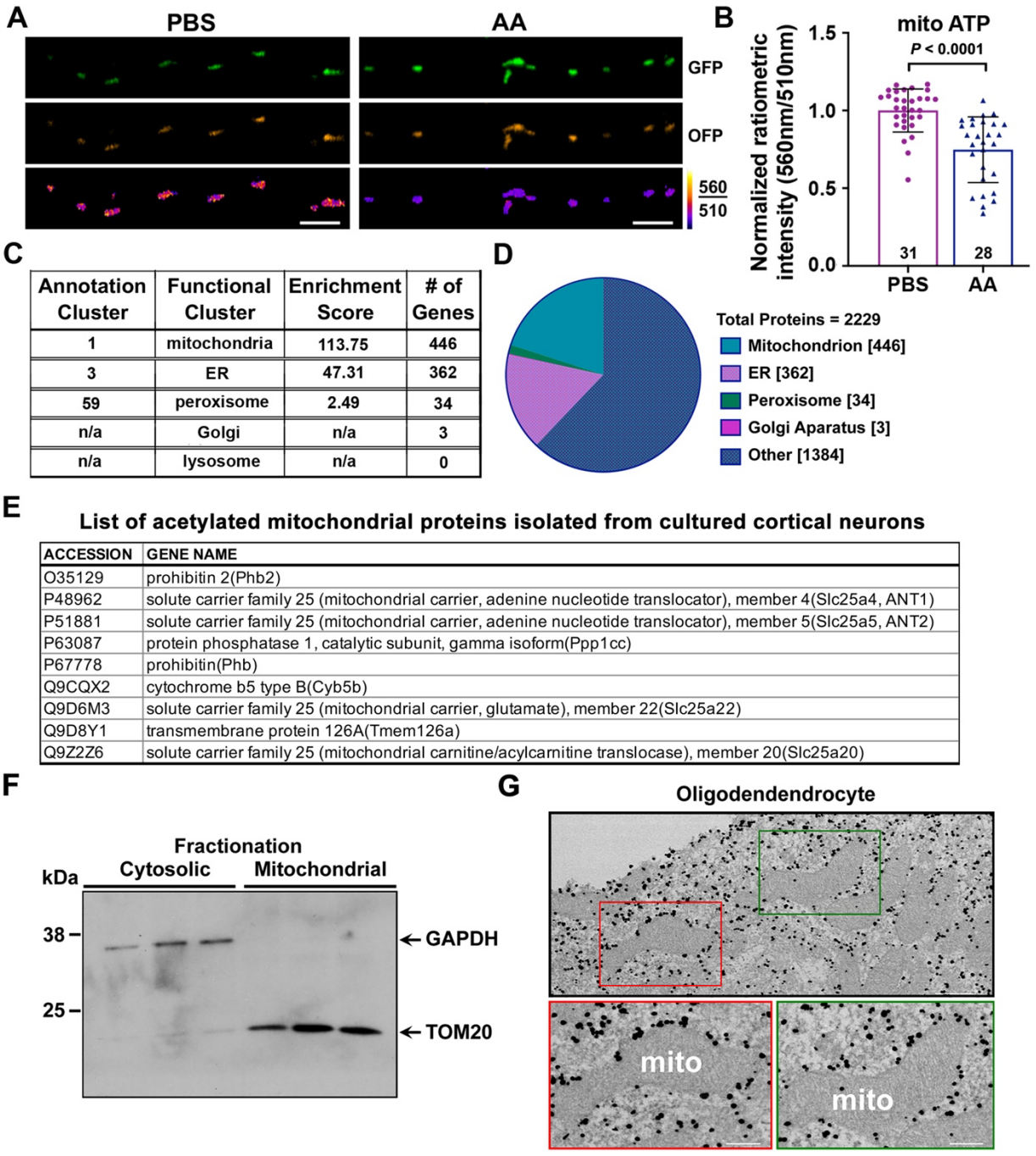

Annotation Cluster	Functional Cluster	Enrichment Score	# of Genes
1	mitochondria	113.75	446
3	ER	47.31	362
59	peroxisome	2.49	34
n/a	Golgi	n/a	3
n/a	lysosome	n/a	0

ACCESSION	GENE NAME
O35129	prohibitin 2(Phb2)
P48962	solute carrier family 25 (mitochondrial carrier, adenine nucleotide translocator), member 4(Slc25a4, ANT1)
P51881	solute carrier family 25 (mitochondrial carrier, adenine nucleotide translocator), member 5(Slc25a5, ANT2)
P63087	protein phosphatase 1, catalytic subunit, gamma isoform(Ppp1cc)
P67778	prohibitin(Phb)
Q9CQX2	cytochrome b5 type B(Cyb5b)
Q9D6M3	solute carrier family 25 (mitochondrial carrier, glutamate), member 22(Slc25a22)
Q9D8Y1	transmembrane protein 126A(Tmem126a)
Q9Z2Z6	solute carrier family 25 (mitochondrial carnitine/acylcarnitine translocase), member 20(Slc25a20)

Figure S6 (related to Figure 6)**. Mitochondrial Protein Acetylation in Cortical Neurons**

(**A, B**) Representative images (**A**) and quantification (**B**) of mitochondrial-targeted ATP sensor GO-ATeam2-Mito, reflecting ATP level in the inner mitochondrial matrix, in DIV8 neuronal axons treated for 24 hours with PBS or AA (5nM). Note that inhibiting mitochondrial respiration with AA significantly reduces inner mitochondrial ATP levels.

(**C, D**) Graphical depiction of mass spectrometry results revealing the most enriched categorizations of 2229 unique proteins identified. Mitochondrial fractions were obtained from DIV7 cortical neurons via differential centrifugation and processed for mass spectrometry. Mitochondrial enrichment was determined by functional annotation of 2229 unique proteins identified using the database for annotation, visualization, and integrated discovery (DAVID). Note that mitochondrial proteins exhibited the strongest enrichment score (113.75), however proteins corresponding to endoplasmic reticulum (ER), peroxisomes, and Golgi apparatus were identified in relatively lower enrichment.

(**E**) Mass spectrometry analyses revealed 9 mitochondrial proteins that were matched to an acetylated peptide sequence on lysine residues under our experimental conditions, thus providing deacetylation candidates of neuronal mitochondrial proteins by SIRT2. A list of acetylated mitochondrial peptides can be found in **Table S1**.

(**F**) Representative western blot demonstrating the relative purity of mitochondrial fractionation via differential centrifugation. The cytosolic protein glyceraldehyde-3-phosphate dehydrogenase (GAPDH) was only detected in the cytosolic fraction (left), while translocase of outer mitochondrial membrane protein 20 (TOM20) was identified in the mitochondrial fraction (right).

(**G**) Electron micrographs of mitochondrial structures (green and red inset boxes) within a DIV5 OL cell. Note the anti-SIRT2 immunogold particles distribute along the mitochondrial membranes in addition to cytosolic staining.

Data were quantified from the total number of axons (**B**) indicated in or below bars and statistical analysis was performed on data collected from three or more biological replicates using an unpaired Student's *t*-test (**B**). Scale bars: 5 μm (**A**), 250 nm (**G**, insets).

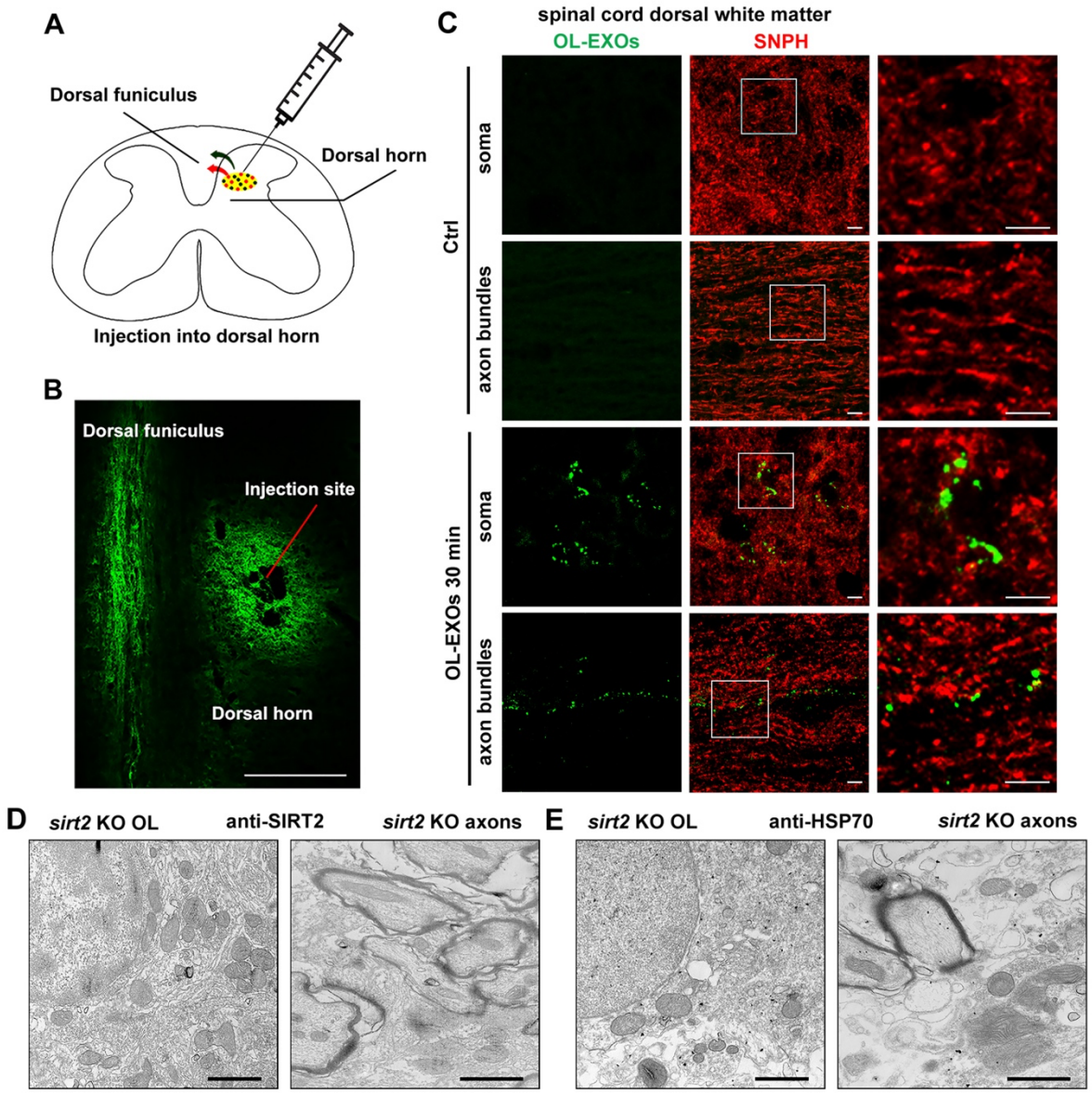

Figure S7 (related to Figure 7)**. Injection of Myelin-Green, CMTMRos and Exosomes into Mouse Spinal Cord**

(**A, B**) Schematic illustration (**A**) and representative image (**B**) show *in vivo* injection of mitochondrial membrane potential dye CMTMRos (3 μl, 10 μM), myelin sheath dye Myelin Green (1:300 dilution), or ExoGlow-labeled OL-EXOs into mouse spinal cord dorsal horn using a 25 μl Hamilton syringe with a 30-gauge needle (point style 4, 30-degree level). After mice were fully anesthetized, a vertical incision was made to expose the T2 spinous process. A laminectomy was performed on the T2 spinous and the underlying dura was exposed. After injection, mice were set to rest for at least 30 minutes to allow dyes or EXOs to diffuse from the injection site to the white matter-enriched dorsal funiculus area, where mitochondrial membrane potential or uptake of ExoGlow-OL-EXOs were examined along myelinated axonal bundles. Mice were perfused and the spinal cord was cut into 3-mm slices above and below the injection site for tissue processing. Note that Myelin Green staining along dorsal funiculus was confirmed by sectioning of the fixed

tissue (**B**). Isolated OL-EXOs released from WT or *sirt2* KO OLs were mixed with the dye cocktail for rescue experiments.

(**C**) Representative images showing uptake of ExoGlow-labeled OL-EXOs (green) into myelinated axon bundles and cell bodies after injection into spinal cord dorsal horn of WT mice. Mice at P60 were anesthetized, followed by a laminectomy performed on the T2 spinous. The spinal cord sections were processed for immunostaining of the neuron-specific and axonal mitochondria-targeted syntaphilin (SNPH) after OL-EXO injection for at least 30 min. Note that uptake of OL-EXOs (green) within SNPH-targeted axon bundles is readily detectable. Enlarged views of the boxed regions are shown on the right.

(**D, E**) Representative immunoelectron micrographs showing SIRT2 (**D**) or HSP70 (**E**) labeling in spinal cord dorsal white matter of *sirt2* KO mice. Note that while HSP70 labeling is readily detectable in both *sirt2* KO OLs and myelinated axons, immunogold SIRT2 signal is undetectable in *sirt2* KO mouse spinal cord without injection of WT OL-EXOs. Scale bars: 100 μm (**B**), 5 μm (**C**), and 1 μm (**D** and **E**).

Table S1 (related to Figure 6)**. List of Acetylated Peptides of Neuronal Mitochondrial Proteins Identified by Mass Spectrometry**

Table S1 (related to Figure 6)**. List of Acetylated Peptides of Neuronal Mitochondrial Proteins Identified by Mass Spectrometry**

Checked	Annotated Sequence	Modifications	Positions in Master Proteins	# Missed Cleavages	Theo. MH+ [Da]	m/z [Da] (by Search Engine): Sequest HT	RT [min] (by Search Engine): Sequest HT	XCorr (by Search Engine): Sequest HT
TRUE	[-].MTDAAVSFAKDFLAGGVAAAISKTAVAPIER.[V]	1xAcetyl [K10]; 1xTMT6plex [K23]; 1xTMT6plex [N-Term]; 1xMet-loss [N-Term]; 1xMet-loss+Acetyl [N-Term]	P51881 [1-31]	2	3447.92518	1149.9763	115.4229	6.14
TRUE	[-].MGDQALSFLKDFLAGGIAAAVSKTAVAPIER.[V]	1xAcetyl [K10]; 1xTMT6plex [K23]; 1xTMT6plex [N-Term]; 1xMet-loss [N-Term]	P48962 [1-31]	2	3516.98302	1172.99288	130.8402	7.2
TRUE	[-].MAAKVFESIGKFGLALAVAGGVVNSALYNVDAGHR.[A]	1xAcetyl [K4]; 1xTMT6plex [K11]; 1xTMT6plex [N-Term]; 1xMet-loss [N-Term]	P67778 [1-35]	2	3902.16926	976.29453	130.2492	6.97
TRUE	[-].MGDQALSFLKDFLAGGIAAAVSK.[T]	1xAcetyl [K10]; 1xTMT6plex [K23]; 1xTMT6plex [N-Term]; 1xMet-loss [N-Term]; 1xMet-loss+Acetyl [N-Term]	P48962 [1-23]	1	2679.51217	1340.25086	137.675	4.91
TRUE	[-].MTDAAVSFAKDFLAGGVAAAISK.[T]	1xAcetyl [K10]; 1xTMT6plex [K23]; 1xTMT6plex [N-Term]; 1xMet-loss [N-Term]	P51881 [1-23]	1	2610.45432	1305.72216	130.0573	4.95
TRUE	[-].MADIDKLNIDSIIQR.[L]	1xAcetyl [K6]; 1xTMT6plex [N-Term]; 1xMet-loss [N-Term]	P63087 [1-15]	1	1885.05921	943.02969	114.2655	4.02
TRUE	[-].MGDQALSFLKDFLAGGIAAAVSKTAVAPIER.[V]	2xAcetyl [K10; K23]; 1xTMT6plex [N-Term]; 1xMet-loss [N-Term]	P48962 [1-31]	2	3329.83066	1110.60753	147.8484	5.57
TRUE	[-].MAQNLKDLAGRLPAGPR.[G]	1xAcetyl [K6]; 1xTMT6plex [N-Term]; 1xMet-loss [N-Term]	O35129 [1-17]	2	1948.12896	650.04532	76.6697	2.82
TRUE	[-].MADKQISLPAK.[L]	1xAcetyl [K4]; 1xTMT6plex [K11]; 1xTMT6plex [N-Term]; 1xMet-loss [N-Term]; 1xMet-loss+Acetyl [N-Term]	Q9D6M3 [1-11]	1	1570.95686	785.97862	79.8962	3.23
TRUE	[-].MESHKPSTSKDDLILNIISR.[K]	1xAcetyl [K5]; 1xOxidation [M1]; 1xTMT6plex [K10]; 1xTMT6plex [N-Term]	Q9D8Y1 [1-20]	1	2800.5279	700.88609	79.5328	3.76
TRUE	[-].MADEPKPISPFK.[N]	1xAcetyl [K6]; 1xTMT6plex [K12]; 1xTMT6plex [N-Term]; 1xMet-loss [N-Term]	Q9Z2Z6 [1-12]	0	1728.99364	864.99517	86.5523	2.79
TRUE	[-].MATPEASGSGEKVEGSEPSVTYYRLEEVAK.[R]	1xAcetyl [K12]; 1xTMT6plex [K30]; 1xTMT6plex [N-Term]; 1xMet-loss [N-Term]	Q9CQX2 [1-30]	2	3570.82156	1190.94346	92.6011	3.25
TRUE	[-].MGDQALSFLKDFLAGGIAAAVSK.[T]	1xAcetyl [K10]; 1xOxidation [M1]; 1xTMT6plex [K23]; 1xTMT6plex [N-Term]	P48962 [1-23]	1	2826.54757	942.84912	146.0138	3.2
TRUE	[-].MAQNLKDLAGR.[L]	1xAcetyl [K6]; 1xTMT6plex [N-Term]; 1xMet-loss [N-Term]	O35129 [1-11]	1	1356.77968	678.89184	74.4921	2.63